

New molecular size estimation in local LIRGs at high-spatial resolution with ALMA.

**Bellocchi, E.¹, Pereira-Santaella, M.¹, Colina, L.¹, Labiano, A.^{1,2},
Sánchez-García, M.^{1,3}, Alonso-Herrero, A.¹, Arribas, S.¹, and García-Burillo, S.³**

¹ Centro de Astrobiología, (CSIC-INTA), Astrophysics Department, Madrid, Spain

² Telespazio UK, for the European Space Agency (ESA), ESAC, Villanueva de la Cañada, Madrid, Spain

³ Observatorio Astronómico Nacional (OAN-IGN)-Observatorio de Madrid, Alfonso XII, 3, 28014 Madrid, Spain

Abstract

We present the first study that provides detailed measurements of the size (i.e., effective radius) of the molecular gas traced by CO(2-1) in a sample of 21 LIRG systems at low- z . To this aim, we used high-resolution ALMA data, which allow us to reach sub kpc spatial resolution scale (<100 pc). The sample encompasses a wide variety of morphological types, suggesting different dynamical phases (isolated spiral galaxies, interacting galaxies, and ongoing and post-coalescence mergers). We performed a comprehensive study of the molecular, stellar, and ionized gas distributions and their relative sizes. Comparison samples of local galaxies and high- z systems have also been included in order to place the low- z LIRGs in a general context.

1 Introduction

The characterization of the distribution of all the ionized, molecular and stellar tracers is key to understanding how the different phases of the interstellar medium (ISM) evolve in size across the cosmic time, studying several types of galaxies, at low- and at high- z . Low- z LIRGs offer a unique opportunity to study extreme star-formation (SF) events at high linear resolution and signal-to-noise ratio (S/N), and compare them with those observed locally (spiral galaxies, early-type galaxies (ETGs), and ULIRGs) and at high- z . In particular, this enables us to compare the size of the host galaxy (stellar component; [1]) with that derived for the ongoing star formation (ionized gas; [2]) as well as the size of the regions where stars are forming (molecular gas) in a local sample of LIRGs and compare them with those derived for local spiral galaxies, ETGs, and ULIRGs as well as high- z star-forming galaxies (SFGs) and sub-millimeter galaxies (SMGs). With the advent of high-resolution instruments such as the Atacama Large Millimeter/Submillimeter Array (ALMA), we are now able to study the

molecular emission in local galaxies at spatial resolutions similar to that covered by typical giant molecular clouds (<100 pc).

2 Sample and observations

The volume-limited sample consists of 21 local LIRGs (24 individual galaxies) at $z \leq 0.02$ for which we obtained ALMA data. The sample has been drawn from the IRAS Revised Bright Galaxy Sample (RBGS, [3]) with distance $D \leq 100$ Mpc. Our LIRGs were previously observed in the optical band using VIMOS/VLT by [4] and ten of them have also been analyzed in the near-IR using SINFONI/VLT data by [5]. We obtained the CO(2–1) line and the continuum at 247 GHz (~ 1.3 mm) emission of a sample of individual local LIRGs observed with ALMA using Band 6 (see Fig. 1) from the projects 2017.1.00255.S (PI: Pereira Santaella, M.), 2015.1.00714.S (PI: Kazimers, S.), 2013.1.00271.S and 2013.1.00243.S (PI: Colina, L.) and 2017.1.00395.S (PI: Díaz-Santos, T.). The synthesized beam full width at half maximum (FWHM) of the sample ranges between $\sim 0.2''$ and $0.4''$. The field of view (FoV) imaged by a single pointing has a diameter ranging between ~ 5 and 8 kpc.

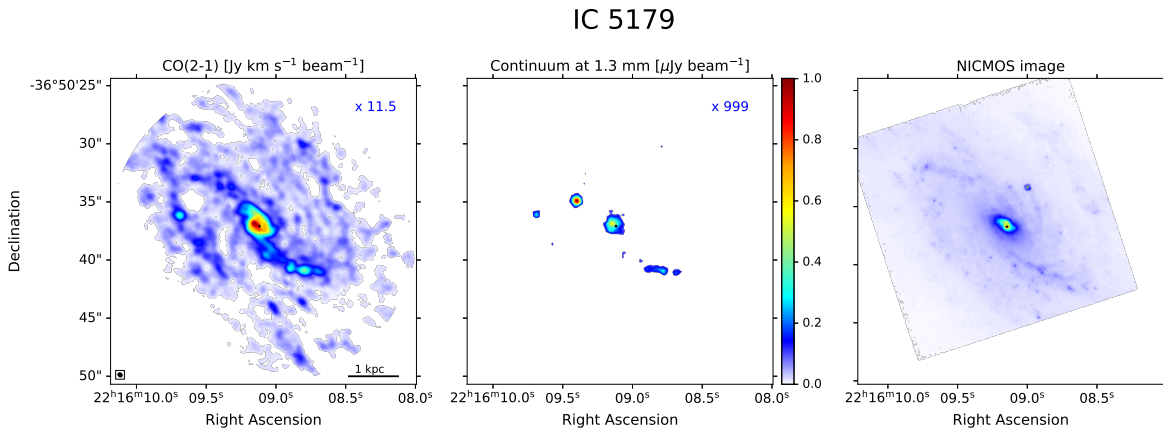


Figure 1: *From left to right*: CO(2–1) and 1.3 mm continuum maps obtained with ALMA, complemented by *HST*/NICMOS image when available. The cross symbol in the three panels represents the stellar peak emission identified using the *HST*/NICMOS image. The beam size and the physical scale in kpc are also shown in the left panel.

3 Data analysis

We generated CO(2–1) and 1.3 mm continuum maps for the whole sample, selecting the emission above 5σ for both maps. To derive the size of a system we consider the curve-of-growth method as a robust way to derive the R_{eff} . We considered an equivalent circular aperture as a good approximation of the (major) elliptical aperture. We select the center of the (circular) aperture, choosing the peak emission observed in the near-IR using *HST*/NICMOS F160W ($\lambda_c = 1.60 \mu\text{m}$, FWHM = $0.34 \mu\text{m}$) images (see Fig. 1, right panel). When the *HST* images are not available, the peak emission in the continuum map at 1.3 mm is used. The CO(2–1)

and 1.3 mm continuum sizes presented in this work are observed (not corrected for the beam). The intrinsic CO and 1.3 mm continuum sizes are also resolved (larger than the beam) and are (on average) smaller than the observed size by $\leq 1\%$ and $\leq 4\%$, respectively.

4 LIRGs versus low- z ETGs, spiral galaxies, and ULIRGs

4.1 SFR versus R_{CO}

LIRGs are completely decoupled from spiral galaxies and ETGs in the SFR- R_{CO} diagram (see Fig. 2, left panel). While spiral galaxies are extended systems with a CO(2–1) radius of about 2 to 10 kpc, LIRGs have radii of about a factor ≤ 6 smaller. Moreover, the sizes of LIRGs cover a range similar to that covered by the sizes of ETGs, while their SFR is a factor 60 higher than for ETGs.

The large discrepancy in the molecular size between spiral galaxies and local LIRGs seems to be in agreement with what is discussed in [6]: these authors found that galaxies that are more compact in the molecular gas than in stars tend to show signs of interaction (the presence of a bar can also affect the emission distribution). The work by [7] seems to support the aforementioned result: these authors derived still more compact molecular size for their sources with respect to our LIRGs. Their sources are more extreme in terms of SFR ($\sim 340 M_{\odot} \text{ yr}^{-1}$) and even show a more disturbed morphology. Their molecular size is a factor 2 more compact than that of our LIRGs.

4.2 Stellar mass versus R_{CO}

In the stellar mass- R_{CO} diagram (Fig. 2, right panel), LIRGs cover a mass range similar to that of low- z samples of spiral galaxies and ETGs, with values in the 10^{10} - $10^{11} M_{\odot}$ range. Compared with different types of low- z galaxies, LIRGs are characterized by being located in galaxy hosts with intermediate stellar mass ($\sim 5 \times 10^{10} M_{\odot}$), forming stars at rates a factor of ≥ 10 above spiral galaxies, and with compact CO sizes ($R_{CO} \sim 0.7$ kpc) similar to those of ETGs ($R_{CO} \sim 1$ kpc).

4.3 Stellar mass–size plane

A different trend from that derived for the stellar mass and molecular size components is derived for our sample when the stellar size is considered (Fig. 3, left panel). As before, local spiral galaxies (i.e., MS SFGs from [8]) and ETGs are included in the diagram. LIRGs share similar stellar mass and stellar size with ETGs, while they are more compact (by a factor ~ 5) and more massive (by a factor ≤ 2) than local MS SFGs. From [9], we know that the distributions of molecular gas and stellar disk in galaxies follow each other closely in nearby disk galaxies ($R_{star} \sim R_{CO}$), while the stellar size is larger than the molecular size for ETGs and for our LIRGs by a factor of ≤ 3 .

According to evolutionary scenarios, many works support the idea that (U)LIRGs can transform gas-rich spiral galaxies into intermediate-(stellar)mass (10^{10} - $10^{11} M_{\odot}$) elliptical

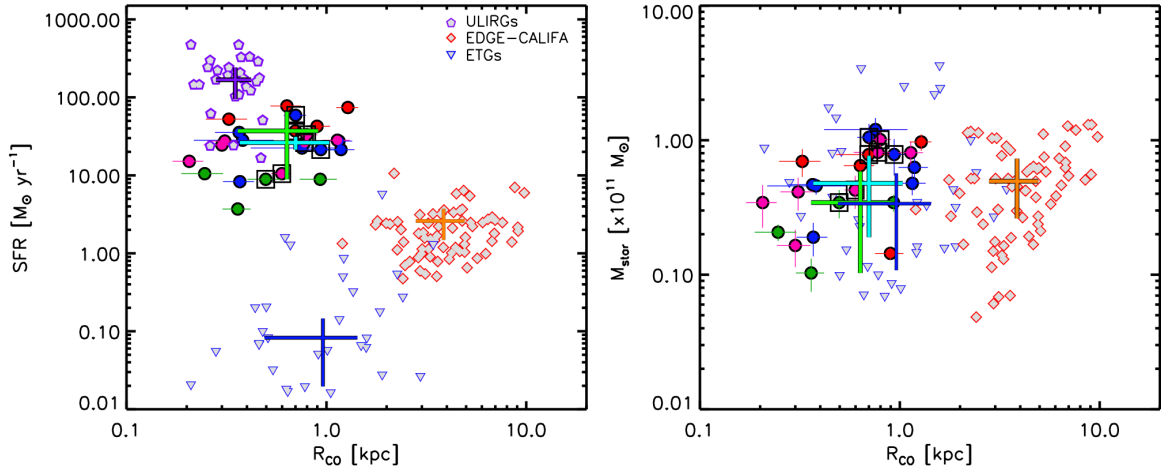


Figure 2: Distribution of LIRGs and other low- z galaxy samples in the SFR– R_{CO} (left) and M_{star} – R_{CO} (right) planes. Our LIRGs are shown using green, magenta and red circles. The median value of each sample is shown according to the following color code: purple for ULIRGs, light green for interacting and merger LIRGs, light blue for disk LIRGs, orange for spiral galaxies, and dark blue for ETGs.

galaxies through merger events ([10]). The kinematic study of local (U)LIRGs ([1]) highlights that these systems fill the gap between rotation-dominated spiral galaxies and dispersion-dominated ETGs in the v/σ – σ plane. Following our present results, most of the LIRGs share similar properties with ETGs while only a few overlap with the region covered by spiral galaxies.

4.4 Stellar hosts in LIRGs *versus* high- z SFGs

A large variety of high- z systems (i.e., MS SFGs, [11], [12], [13], [14], [15], [16], [17], [18] and SMGs, [19], [20], [21], [22], [23]) were selected using different criteria (i.e., stellar mass, optical radius, or IR luminosity) and observational techniques also covering a broad range of redshifts ($1 \leq z \leq 6$) and galaxy properties. Therefore, they represent the rich diversity of galaxies found during the first half of the history of the Universe. The vast majority of high- z galaxies have masses in the $\sim 10^{10}$ – $2 \times 10^{11} M_{\odot}$ mass range, but their sizes cover a much wider range, which reflects the large variety of systems considered at high- z (Fig. 3, right panel).

The comparison with MS SFGs indicates that low- z LIRGs have stellar sizes and masses similar to those of K-band-selected SFGs at redshifts 3–4 ([11]). However, LIRGs appear (on average) slightly smaller in size (factor 1.3) than the MS SFGs at $z \sim 1$ –2 (e.g., [13], [17], [18]) while their masses (average of $5.6 \times 10^{10} M_{\odot}$) are within the wide range of stellar masses (from 4.3 to $20.0 \times 10^{10} M_{\odot}$) covered by the hosts of the MS SFGs. These results indicate that LIRGs, which represent the bursty above-MS SFGs at low- z , appear to be similar to the bulk population of MS SFGs at intermediate redshifts ($z \sim 1$ –4) in terms of the stellar mass

and size of their hosts.

All the low- z LIRGs, as well as a large fraction of the high- z galaxies, appear in the stellar mass–size diagram (Fig. 3, right panel) in between the relations of early- and late-type galaxies at $z \sim 1.75$ (typical redshift value for the majority of the high- z systems considered in this work), as derived from the *3D-HST* and *CANDELS* surveys ([24] and references therein). As observed in local LIRGs, distant SMG populations also show a mixture of dynamical phases, hosting merger-driven starbursts ([25]) as well as ordered rotating disks ([19]). This could indicate that many of the high- z galaxies could be in a transitory phase related to tidally perturbed disks or galaxies involved in interactions and mergers, such as low- z LIRGs. Deciphering whether or not this transitory phase represents the evolution from extended disks to compact spheroids requires spatially resolved kinematical information traced by the molecular and ionized ISM.

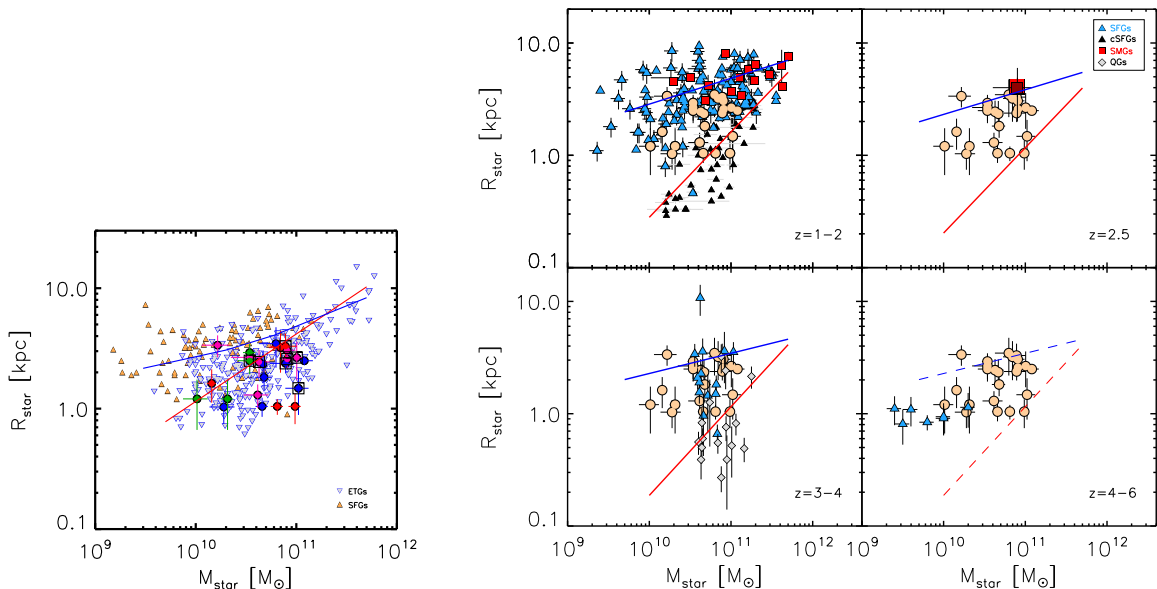


Figure 3: *Left*: Mass–size distribution for our LIRGs including ETGs and local spiral galaxies (i.e., MS SFGs; [8]). LIRGs are identified following the color code used in previous figures. The blue and red slopes represent the mass–size relations derived by [26] for late- and early-type local galaxies, respectively. *Right*: Mass–size distribution for our LIRGs and high- z systems. LIRGs from this work are shown using light orange circles. High- z SFG and SMG data are taken from the following works: SMGs from [19], [20], [21], and [22] and SFGs from [11], [12], [13], [14], [15], [16], [17], and [18]. The blue and red lines in each redshift range represent the mass–size relations for late- and early-type galaxies, respectively, at $z \sim 1.75$, 2.25, and 2.75 derived from the *3D-HST*+*CANDELS* surveys ([24]). At $z=4-6$, the mass–size relation for late- and early-type galaxies has not yet been derived, and so the dashed blue and red lines still show the behavior considered at $z=3-4$.

Acknowledgments

This research was supported from the Comunidad de Madrid through the Atracción de Talento grant 2017-T1/TIC-5213. This research has been partially funded by the Spanish State Research Agency (AEI) Project MDM-2017-0737 Unidad de Excelencia ‘María de Maeztu’- Centro de Astrobiología (INTA-CSIC). EB also acknowledges financial support from the María Zambrano program of the Spanish Ministerio de Universidades funded by the Next Generation European Union and partly supported by the grant RTI2018-096188-B- I00 funded by MCIN/AEI/10.13039/501100011033.

References

- [1] Bellocchi, E., Arribas, S., & Colina, L. 2016, *A&A*, 591, A85
- [2] Arribas, S., Colina, L., Alonso-Herrero, A., et al., 2012, *A&A*, 541, 20
- [3] Sanders, D. B., Mazzarella, J. M., Kim, D. C., Surace, J. A., & Soifer, B. T. 2003, *AJ*, 126, 1607
- [4] Arribas, S., Colina, L., Monreal-Ibero, A., et al., 2008, *A&A*, 479, 687
- [5] Crespo Gómez, A., Piqueras López, J., Arribas, S., et al. 2021, *A&A*, 650, A149
- [6] Bolatto, A. D., Wong, T., Utomo, D., et al. 2017, *ApJ*, 846, 159
- [7] Pereira-Santaella, M., Colina, L., García-Burillo, S., et al. 2021, *A&A*, 651, A42
- [8] Leroy, A. K., Schinnerer, E., Hughes, A., et al. 2021, *ApJS*, 257, 43
- [9] Leroy, A. K., Walter, F., Sandstrom, K., et al. 2013, *AJ*, 146, 19
- [10] Cappellari, M., McDermid, R. M., Alatalo, K., et al. 2013a, *MNRAS*, 432, 1862
- [11] Straatman, C. M. S., Labbé, I., Spitler, L. R., et al. 2015, *ApJ*, 808, L29
- [12] Tadaki, K.-I., Genzel, R., Kodama, T., et al. 2017, *ApJ*, 834, 135
- [13] Förster Schreiber, N. M., Renzini, A., Mancini, C., et al. 2018, *ApJS*, 238, 21
- [14] Puglisi, A., Daddi, E., Liu, D., et al. 2019, *ApJ*, 877, L23
- [15] Cheng, C., Ibar, E., Smail, I., et al. 2020, *MNRAS*, 499, 5241
- [16] Kaasinen, M., Walter, F., Novak, M., et al. 2020, *ApJ*, 899, 37
- [17] Valentino, F., Daddi, E., Puglisi, A., et al. 2020, *A&A*, 641, A155
- [18] Puglisi, A., Daddi, E., Valentino, F., et al. 2021, *MNRAS*, 508, 5217
- [19] Hodge, J. A., Swinbank, A. M., Simpson, J. M., et al. 2016, *ApJ*, 833, 103
- [20] Chen, C.-C., Hodge, J. A., Smail, I., et al. 2017, *ApJ*, 846, 108
- [21] Calistro Rivera, G., Hodge, J. A., Smail, I., et al. 2018, *ApJ*, 863, 56
- [22] Lang, P., Schinnerer, E., Smail, I., et al. 2019, *ApJ*, 879, 54
- [23] Chen, C.-C., Harrison, C. M., Smail, I., et al. 2020, *A&A*, 635, A119
- [24] van der Wel, A., Franx, M., van Dokkum, P. G., et al. 2014, *ApJ*, 788, 28
- [25] Aguirre, P., Baker, A. J., Menanteau, F., Lutz, D., & Tacconi, L. J. 2013, *ApJ*, 768, 164
- [26] Shen, S., Mo, H. J., White, S. D. M., et al. 2003, *MNRAS*, 343, 978